JOURNAL OF MATERIALS SCIENCE 14 (1979) 2741–2746

TEM studies on $Al_4C_3 \cdot 3Be_2C$

A. ZANGVIL*, L. J. GAUCKLER†, G. SCHNEIDER, M. RÜHLE
Max-Planck-Institut für Metallforschung, Institut für Werkstoffwissenschaften, Stuttgart, Germany

X-ray diffraction studies and TEM investigations of the binary $Al_4C_3 \cdot 3Be_2C$ alloy (prepared at 1860° C) revealed that besides the matrix platelets of Be_2C and an additional third phase are also present. From XRD the lattice parameter of the cubic phase was found to be 0.4612 nm. Small additions of SiC stabilize the cubic phase forming solid solution by partial replacement of Al^{3+} by Si^{4+}. This replacement causes a decrease of the lattice parameter to 0.4565 nm.

1. Introduction

Three intermediate phases exist at 1860° C in the system Al_4C_3–Be_2C with the molar ratio (Al_4C_3 : Be_2C) of 3:1, 1:1, and 1:3, respectively [1]. The $Al_4C_3 \cdot 3Be_2C$ specimens (molar ratio 1:3) consist mainly of a cubic phase, but also traces of Be_2C were observed, even after preparation at a temperature of 2060° C [1, 2]. However, single phase cubic solid solutions could be prepared after adding 3 to 6 mol % SiC to the binary composition, c.f. Fig. 1. The solid solution range is described by

$$Al_2Be_{3-4x}Si_{2x}C_3$$

for $x = 0.03$ to 0.06. About 2 mol % Be_2C can also be dissolved in the cubic structure in excess of the exact 1:3 ratio.

Microstructural features of the binary and ternary compositions of $Al_4C_3 \cdot 3Be_2C$ are shown in this paper. They were obtained by transmission electron microscopy (TEM) studies. The observations are compared with results of other investigations, mainly with X-ray diffraction studies (XRD).

2. Experimental details

Specimens were hot-pressed in graphite dies at 1860° C and 2060° C, respectively, and at 30 MN m^{-2} [2] using mixtures of Al, Be, Si and C (graphite) powders. X-ray diffraction studies (XRD) were performed with a Philips goniometer fitted with a double bent LiF-monochromator using CuKα radiation at 40 kV. Specimens transmittable for TEM studies were prepared in the standard way by diamond-wheel cutting, mechanical polishing and ion beam milling. A gold or carbon layer of about 5 nm thickness was evaporated onto the specimens to avoid electrical discharging. All TEM studies were performed with a JEM 200A microscope operated at 200 kV. The microscope was fitted with a double tilting stage.

3. Experimental results

XRD studies were performed prior to the TEM observations. The results of XRD are summarized in Table I for the multiphase binary (MPB, composition: $Al_4C_3 \cdot 3Be_2C$) and the single phase ternary (SPT composition: $Al_4C_3 \cdot 3Be_2C$ + 4.5 mol % SiC). Cubic phases were analysed for the MPB and SPT materials by XRD. The lattice parameters were 0.4612 nm (MPB) and 0.4565 nm (SPT), respectively. However, in the MPB alloy diffraction lines from the (cubic) Be_2C phase could also be observed.

TEM studies were performed on both alloys. Fig. 2 shows a typical micrograph of the MPB alloy. The different phases can be observed easily. Each grain of the $Al_4C_3 \cdot 3Be_2C$ matrix contains platelets of a second phase. The thicknesses of the

*Present address: Department of Metallurgy and Mining Engineering, University of Illinios, Urbana, Illinios 61801, USA.

†Present address: Swiss Aluminium Ltd., Research and Development, CH-8212 Neuhausen, Switzerland.

0022–2461/79/112741–06 $02.60/0

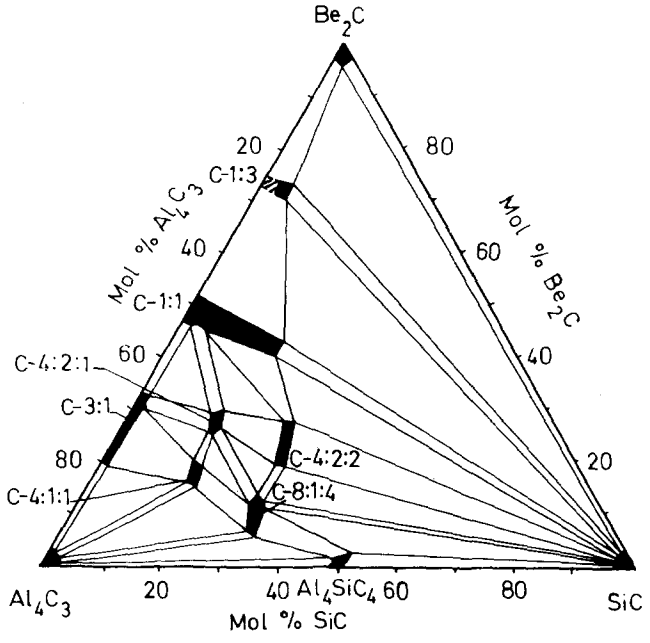

Figure 1 Phase equilibrium of the system Al_4C_3–Be_2C–SiC at 1860° C [1].

Phase	Composition
C-3:1	$3Al_4C_3 \cdot Be_2C$
C-1:1	$Al_4C_3 \cdot Be_2C$
C-1:3	$Al_4C_3 \cdot 3Be_2C$
C-4:1:1	$4Al_4C_3 \cdot Be_2C \cdot SiC$
C-4:2:1	$4Al_4C_3 \cdot 2Be_2C \cdot SiC$
C-4:2:2	$4Al_4C_3 \cdot 2Be_2C \cdot 2SiC$
C-8:1:4	$8Al_4C_3 \cdot Be_2C \cdot 4SiC$

platelets are about 20 to 40 μm. Fig. 3a shows a typical selected area diffraction (SAD) diagram of the MPB alloy. The main reflections could be identified to be caused by a cubic structure. However, each reflection (Fig. 3a) was split into 2 sub-reflections. The correlated reflections are always co-radial, with the reflections with the smaller diffraction vectors (larger lattice parameter) belonging to the cubic phase of the matrix, while those with the larger diffraction vectors are caused by the Be_2C phase. Since the equivalent reflections were always co-radial it can be concluded that the basis vectors of the unit cells of both structures are parallel.

TABLE I Indexed XRD of the binary and ternary cubic phase $Al_4C_3 \cdot 3Be_2C$/SiC and unindexed *d*-values of the precipitates (Y-phase).

Phase	$Al_4C_3 \cdot 3Be_2C$ multiphase				$Al_4C_3 \cdot 3Be_2C$ + 4.5 mol% SiC	
	Measured			Calculated *d* (nm) with $a_0 = 0.4612$ nm	Measured *d* (nm)	Calculated *d* (nm) with $a_0 = 0.4565$ nm
	h k l	*d* (nm)	J/J_0			
$Al_4C_3 \cdot 3Be_2C$	1 1 1	0.2661	100	0.2663	0.265	0.2636
Be_2C	1 1 1	0.2513	15			
Y		0.2342	10			
$Al_4C_3 \cdot 3Be_2C$	2 0 0	0.2301	23	0.2306	0.2285	0.2283
Y		0.2055	7			
Y		0.1719	5			
Y		0.1675	15			
Y		0.1664	15			
$Al_4C_3 \cdot 3Be_2C$	2 2 0	0.1629	60	0.1631	0.1617	0.1614
Be_2C	2 2 0	0.1535	9			
Y		0.1411	9			
$Al_4C_3 \cdot 3Be_2C$	3 1 1	0.1391	15	0.1391	0.1377	0.1376
Y		0.1365	5			
$Al_4C_3 \cdot 3Be_2C$	2 2 2	0.1330	5	0.1331	0.1318	0.1318
Y		0.1176	4			
$Al_4C_3 \cdot 3Be_2C$	4 0 0	0.1154	5	0.1153	0.1141	0.1141
$Al_4C_3 \cdot 3Be_2C$	3 3 1	0.1057	5	0.1058	0.1047	0.1047
$Al_3C_3 \cdot 3Be_2C$	4 0 2	–	–	0.1031		
Y		0.0952	4			
$Al_4C_3 \cdot 3Be_2C$	4 2 2	0.0942	5	0.0941		

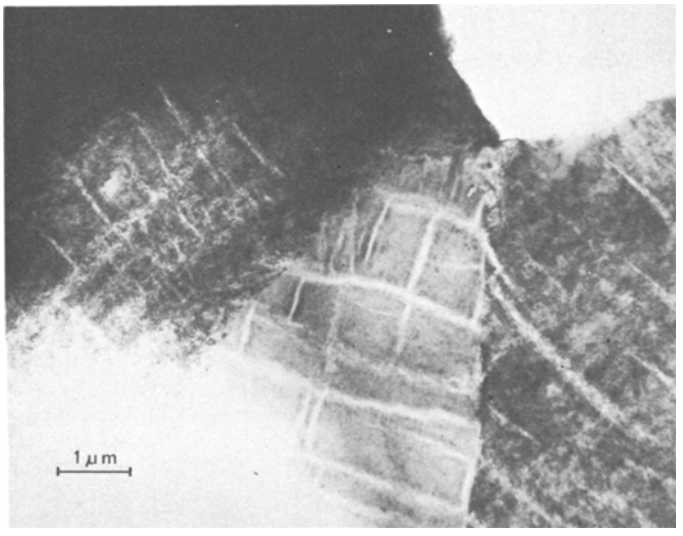

Figure 2 TEM micrograph of the multi-phase binary alloy $Al_4C_3 \cdot 3Be_2C$. The bright areas are platelets of Be_2C.

Besides the matrix reflections (indicated by P) and reflection of the cubic Be_2C phase (indicated by B), weak additional reflection (indicated by Y) could always be observed. Figs. 3b, c and d are dark-field micrographs taken with a matrix reflection P (Fig. 3b), a platelet reflection B (Fig. 3c), and with one of the very weak reflections Y (Fig. 3d). From Fig. 3d it can be concluded that the $Al_4C_3 \cdot 3Be_2C$ grains themselves contain fine precipitates shaped like discs of platelets on {1 0 0} planes. Their diffraction patterns indicate coherency of the precipitates with the matrix. However, their structure could not be resolved; presumably since many of the reflections coincide with those of the $Al_4C_3 \cdot 3Be_2C$ grains. The non-indexed diffraction lines of Table I, designated as Y, are attributed to those precipitates since no other crystalline phase was observed in the specimen.

Single phase samples of the ternary system (SPT) could be prepared by dissolving 3 to 6 mol% SiC in $Al_4C_3 \cdot 3Be_2C$ during the preparation. These solid solutions, designated SPT, have smaller lattice parameters than the phase without Si (MPB). From XRD of a specimen containing 4.5 mol% SiC a refined lattice parameter of 0.4565 ± 0.0001 nm was obtained. This lattice parameter is about 1% smaller than that of the Si-free material (0.4611 nm).

The SPT system (solid solution) has several interesting microstructural features. The grains are divided into sub-grains by low angle grain boundary dislocation networks (Fig. 4). The sub-grains are only a few μm in diameter. The sub-grains may act as nucleation sites for precipitates, as will be shown later. In addition, domain boundaries appear inside the sub-grains, as shown in Figs. 4a and 5a. There are (i) tetrahedral domains bounded by stacking faults on the {1 1 1} planes and (ii) zig-zag boundaries which, in general, do not lie on particular crystallographic planes. These zig-zag boundaries are either anti-lattice boundaries or inversion boundaries. No superlattice reflections resulting from a superstructure were observed. On the other hand, strong diffuse scattering was found on SAD patterns, as shown in Fig. 5b. Dark-field images which were taken by using the diffuse intensity region of the SAD could not reveal any feature within the domains. From this we exclude the possibility of micro-domains larger than about 1 nm, which was the resolution limit. The diffuse "streaks" in Fig. 5b which are pointing out from the (1 1 1) reflection, indicate, if interpreted kinematically, short range ordering (SRO) along the cubic edges with a range of 0.8 to 2 nm (2 to 5 unit cells).

Fig. 5a, and the weak beam dark-field image (Fig. 4b) in particular, show clearly that the boundary can be free of any precipitates. In some regions of the same type of specimens, however, precipitation started on some of the boundaries, as can be seen in the upper part of Fig. 6a. Small rectangular particles, identified as Be_2C, appear between the dislocation lines. These are actually long thin strips, bounded by dislocation lines along their long dimension and lying in the sub-boundary surface, forming a continuous thin layer. Strong coherency strains are observed in the matrix and

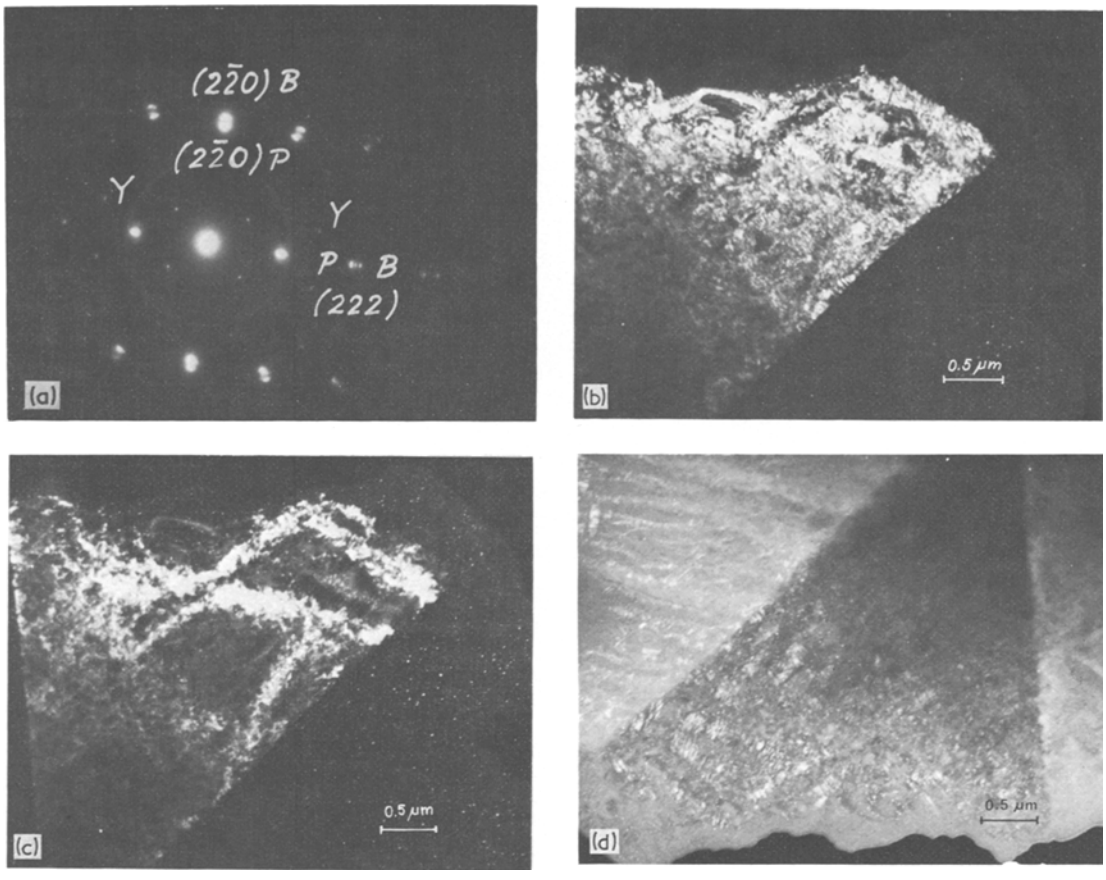

Figure 3 (a) Selected area diffraction (SAD) and dark-field electron micrographs of the multiphase binary $Al_4C_3 \cdot 3Be_2C$ alloy. Different diffraction vectors are used for imaging the same area. (b) Diffraction vector $g_1 = (2\,\bar{2}\,0)$ of the matrix P; (c) diffraction vector $g_2 = (2\,2\,2)$ of a Be_2C B; (d) diffraction vector g_3 of a reflection of the fine precipitates Y. The rings on the SAD in (a) are caused by a thin gold layer evaporated onto the specimen.

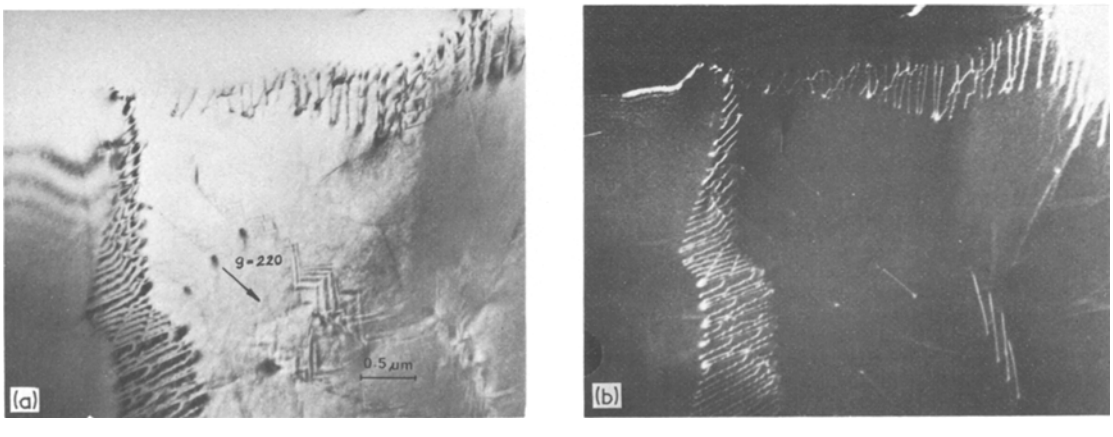

Figure 4 TEM bright-field and weak beam dark-field micrographs of the ternary $Al_4C_3 \cdot 3Be_2C$ + 4.5 mol% SiC specimen. Dislocations of low angle boundaries can be seen easily.

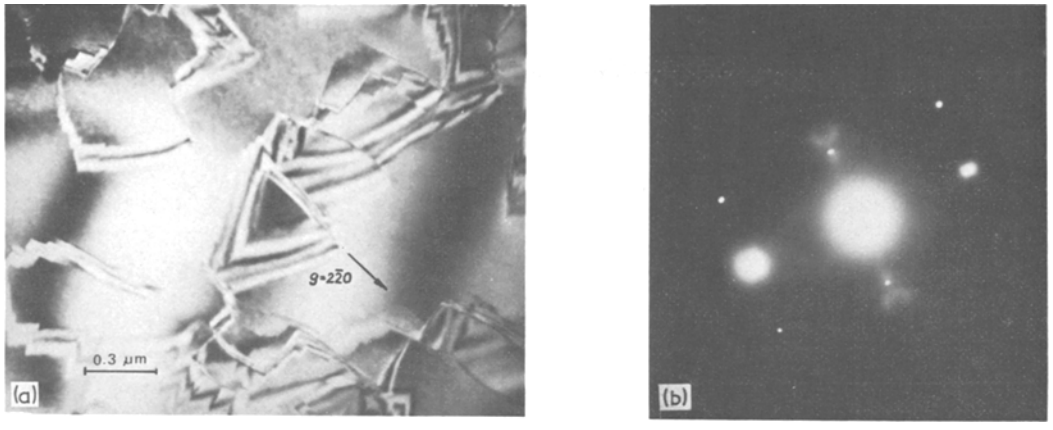

Figure 5 (a) TEM dark-field micrograph of $Al_4C_3 \cdot 3Be_2C$ + 4.5 mol% SiC. Tetrahedral domain boundaries with stacking faults on (1 1 1) planes are visible. (b) SAD of Fig. 5a. Diffuse scattering can be observed.

within the precipitates. This can be interpreted as an early stage of the precipitation process. Precipitation is further advanced in another part of the same specimen (see e.g. Fig. 6b).

4. Discussion

In the binary system Al_4C_3–Be_2C, the $Al_4C_3 \cdot 3Be_2C$ phase could never be obtained pure; there were always platelets of Be_2C present. By XRD studies a single phase could be analysed in the ternary system which was obtained by adding SiC. However, the TEM studies revealed that small Be_2C particles could also be present in the ternary system. The particles were mainly located at the dislocation networks of small angle grain boundaries.

In addition, Y-phase precipitates appeared inside the grains of the binary $Al_3C_3 \cdot 3Be_2C$ samples (MPB). The appearance of three phases in the MPB samples at the same time is a characteristic feature of a non-equilibrium state. This state is assumed to be formed during the cooling process. Be_2C, which precipitates from the cubic $Al_4C_3 \cdot 3Be_2C$ phase changes the composition of the specimen towards higher Al_4C_3 concentration. On further cooling, an additional phase Y inside the cubic grains is formed. Therefore, we assume that the composition of Y must be enriched with Al compared to the cubic phase, i.e. the Y phase lies in the phase diagram (Fig. 1) between $Al_4C_3 \cdot 3Be_2C$ and $Al_4C_3 \cdot Be_2C$.

The observed lattice parameter of the cubic $Al_4C_3 \cdot 3Be_2C$ phase decreased on dissolving SiC. This can be explained by the assumption that some of the Al atoms are replaced by Si atoms. This replacement results in the observed decrease of the lattice parameter, since the radius of Si atoms is smaller than that of Al.

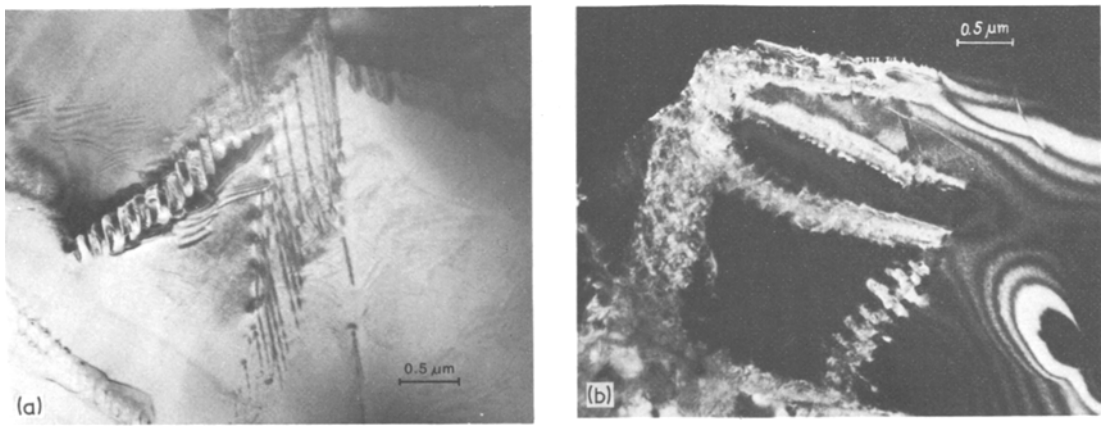

Figure 6 TEM micrographs of $Al_4C_3 \cdot 3Be_2C$ + 4.5 mol% SiC with Be_2C precipitates. (a) Bright-field image; (b) dark-field image.

The binary $Al_4C_3 \cdot 3Be_2C$ phase has a cubic lattice with a lattice parameter of 0.4611 nm. If we assume that the density of the MPB alloy lies between that of Be_2C (2.435 g cm^{-3} [3]) and that of $Al_4C_3 \cdot Be_2C$ (calculated as 2.85 g cm^{-3} [4]) then the unit cell contains $z = 1.23$ to 1.44 of the chemical unit formula $Al_zBe_3C_3$. The other structures occurring in this system are hexagonal. We conclude that our phase is built up like the other structures of this system by carbon atom layers with metal atoms occupying intermediate layers. Therefore the equivalent hexagonal unit cell would contain three carbon atoms, and have $\frac{3}{4}$ the volume of the cubic unit cell. This implies a z value of 1.33 for the cubic cell, corresponding to a composition $Al_{8/3}Be_4C_4$, implying a density of 2.654 g cm^{-3}. If the four carbon atoms occupy the corners and the face centres of the cube as in Be_2C, then it is likely that the Al atoms occupy octahedral sites [3]. However, only $\frac{8}{3}$ of the four possible sites are occupied on average. In consequence, beryllium ions probably occupy the tetrahedral sites. It cannot be decided whether only the four "regular" tetrahedral sites, as in the wurtzite structure, are occupied or if all 8 sites are utilized (as in Be_2C) with partial occupation and with a possible ordering. The diffuse scattering observed in the ternary composition, which implies a SRO along directions parallel to the cube edges, seems to favour the second possibility, because neighbouring tetrahedral sites are indeed arranged along ⟨1 0 0⟩ directions. The SRO is about 2 to 5 unit cells in these directions.

5. Conclusions

(1) Binary compositions at $Al_4C_3 \cdot 3Be_2C$ mainly consist of a cubic material with $a_0 = 0.4612$ nm and include (i) precipitates of Be_2C and (ii) an Al-rich phase.

(2) An addition of 3 to 6 mol% SiC to $Al_4C_3 \cdot 3Be_2C$ stabilized the cubic phase with $a_0 = 0.4572 \pm 0.0005$ nm.

(3) For the binary cubic phase, a unit cell formula of $Al_{8/3}Be_4C_4$ is suggested. C atoms may occupy f c c positions, Be atoms the tetrahedral sites, and Al the octahedral sites, respectively.

(4) The general formula for the ternary solid solution starting at $Al_4C_3 \cdot 3Be_2C$ is $Al_{4z}Be_{6z}Si_{4-6z}C_4$ with a z-value of 0.645 to 0.667 at 1860° C.

Acknowledgement

Thank is due to Professor Dr G. Petzow for his steady interest in this work and to the Bundesministerium für Forschung und Technologie of the Federal Republic of Germany for financial support.

References

1. G. SCHNEIDER, L. J. GAUCKLER, G. PETZOW and A. ZANGVIL, *J. Amer. Ceram. Soc.* (to be published).
2. G. SCHNEIDER, Ph.D. thesis, University of Stuttgart (1978).
3. STARITZKY, *Anal. Chem.* 28 (1956) 915.
4. A. ZANGVIL, L. J. GAUCKLER and G. SCHNEIDER, to be published.

Received 4 April and accepted 11 May 1979.